**SPE Brazil Flow Assurance Technology Congress**
Rio de Janeiro, Brazil, November 06 – 08 2024

# Scrutinizing Atypical Phase Behavior of $CO_2$ with n-hexadecane: Miscibility Window and Mass Barotropy

Danilo A. Ribeiro[1,2*], Rafael M. Charin[1,3], Alexandre J.M. Vieira[2], Krishnaswamy Rajagopal[1,2]

[1]Universidade Federal do Rio de Janeiro, Brazil
[2]Escola de Química - UFRJ, Laboratório de Termodinâmica e Cinética Aplicada (LATCA), Brazil
[3]Escola Politécnica - UFRJ, Brazil
*Email of corresponding author: dandrade@eq.ufrj.br

## Abstract

The investigation of phase behavior in systems rich in carbon dioxide ($CO_2$) is of great interest to the oil and gas industry, especially given the Brazilian pre-salt scenario, where the reserves have significant concentrations of $CO_2$ in the associated gas. This has a strong relationship with techniques that mitigate the environmental problems caused by the discharge of this gas into the atmosphere, such as carbon capture and storage (CCS). $CO_2$ has specific properties that can induce unusual phase behavior, under certain conditions, in mixtures containing hydrocarbons. Understanding these unusual behaviors, observed both in the laboratory and in field samples, is fundamental. In a visual PVT cell, experiments on high-pressure phase equilibrium using a model system containing $CO_2$ and n-$C_{16}H_{34}$ were conducted. The mixture of n-hexadecane with analytically pure $CO_2$ was prepared in different $CO_2$ molar ratios (57.14%, 83.06%, 86.53% and 94.18%). During the study, liquid-liquid (LL), vapor-liquid (VL) and vapor-liquid-liquid (VLL) phase transitions were observed. Specially, the miscibility window displayed by such complex phase behavior around the temperature of 25 ºC was scrutinized. At pressures inside LL boundaries, a turbid region evidences no separation between the phases due to low interfacial tension and similar densities. The main objective of this study is to describe unusual phase behaviors that high $CO_2$ content mixtures can show under high-pressure.

## Keywords

$CO_2$ phase behavior; Barotropy; Ultra-Low Interfacial Tension Region.

## Introduction

Reducing carbon dioxide emissions into the atmosphere is essential due to the growing environmental concerns, especially related to global warming. Considering that most of Brazil's pre-salt reservoirs contain high concentrations of $CO_2$, it becomes imperative to find suitable solutions for this compound. An intuitive approach, which also offers favorable results in terms of recovery, is the reinjection of $CO_2$ into the reservoirs. Increasing the efficiency of recovering reserves by injecting $CO_2$-rich streams is the main objective in tertiary or enhanced oil recovery processes (EOR) [1]. Carbon capture and storage (CCS) stands as a crucial technology in the efforts against severe climate changes, offering a promising means to mitigate $CO_2$ emissions. Nevertheless, it brings several complexities, particularly in understanding the behavior of carbon-dioxide-rich phases.

$CO_2$ has specific properties that can induce exotic phase behavior in oil mixtures under specific conditions. Therefore, the proper understanding of these phase behaviors in systems with high $CO_2$ concentrations is imperative for the efficient production of the Brazilian pre-salt as well as carbon capture and storage processes. Furthermore, such knowledge can help high-pressure separator design.

The phase behavior investigations on $CO_2$, when used in EOR processes, was explored in a study carried out in 1983[5]. In this paper, the authors portray the miscibility window of $CO_2$ in oil and reports the phases that do not separate due to small difference in density between them and low interfacial tension. The presence of liquid-liquid equilibrium and three-phase liquid-liquid-vapor equilibrium was observed in the test carried at 41 °C[5].

In this study, a Schlumberger® visual PVT cell was used to analyze the high-pressure phase equilibrium of a model system containing $CO_2$ and n-hexadecane. This mixture was chosen due to its well-known atypical behavior regarding miscibility window and mass barotropy (density inversion). The PVT visual analysis was conducted under equilibrium conditions at a constant temperature of 298.15K and pressures up to 80 MPa (11.603 Psi). During the study, liquid-liquid (LL), vapor-liquid

(VL) and vapor-liquid-liquid (VLL) phase transitions were observed.

This work scrutinizes the region close to LL saturation pressures, at a constant temperature of 298.15K, which is characterized by low interfacial tension between the coexisting phases in the system, making it difficult to separate them, and similar density with the mass barotropy phenomena.

## Methodology

A Schlumberger PVT visual cell was used to examine the phase behavior of mixtures of n-hexadecane and $CO_2$ in different compositions. Using a cylindrical piston positioned at the top of the cell, saturation pressures were measured at a specified temperature of 25°C. The experimental method was based on constant composition expansion (CCE) procedure.

### Visual thermodynamic equilibrium cell

The equilibrium cell is a device designed to characterize the phase behavior of fluids under different temperature and pressure conditions. It has a maximum working volume of 80 $cm^3$ and can operate in extreme conditions of up to 100 MPa and from -10 to 180°C, as specified in the manufacturer's manual. The Visual Thermodynamic Equilibrium Cell used in this study was manufactured by Schlumberger. This cell is capable of monitoring and controlling changes in Pressure, Volume and Temperature (PVT) and is used, among other applications, to determine bubble and dew points, identify the retrograde condensation region of gaseous hydrocarbons mixtures, and measure the specific masses and relative volumes between the phases in equilibrium as a function of pressure and temperature. The PVT cell, main component of the equipment, is a cylindrical borosilicate glass tube, positioned inside a steel jacket with two sapphire windows on opposite sides. This glass cylinder must be carefully fitted inside the steel jacket, as it is quite fragile and susceptible to fractures and breaks. The space between the glass cylinder and the steel guard is filled with colorless mineral oil, which acts as an internal pressurizing and encapsulating fluid.

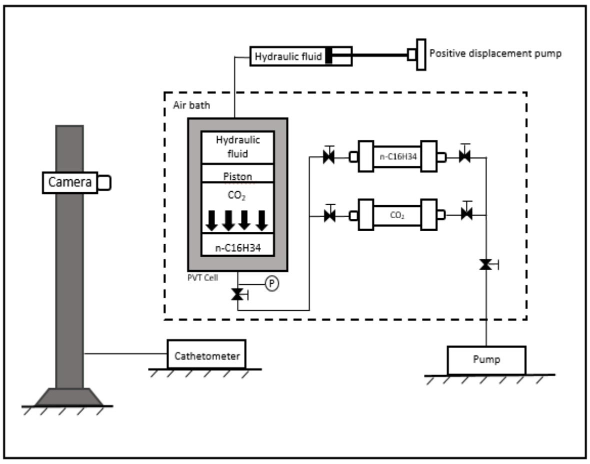

Figure 1. Main components of the PVT cell
Source: elaborated by the author (2024)

A set consisting of a camera coupled to a cathetometer is positioned in front of the viewing window of the PVTcell. The cathetometer is connected to a level controller and the camera to a high-definition monitor, as shown in fig. (2). Using this monitor, measurements are taken of the relative positions of the sample in relation to the base of the glass cylinder height (where the height is set to zero), and thus the volume of the sample is recorded.

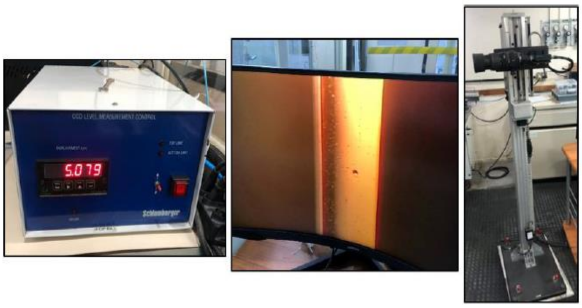

Figure 2. (a) Level controller, (b) monitor for image display, and (c) catheter and camera assembly
Source: LATCA/EQ/UFRJ

### Experimental Procedure

The n-hexadecane stored in the floating-piston-cylinder at a pressure of 2.07 MPa is transferred to the PVT cell. Once the injection is complete, the pressure at which the pure n-hexadecane is confined is increased to 27.6 MPa, and then the $CO_2$ is injected at constant pressure. This pressure value is high enough to ensure that the $C_{16}$ and $CO_2$ mixture is single-phase during and after injection, based on data in the literature on the miscibility window of this system [3, 4]. The mixer is always kept on to ensure the mixture is homogeneous.

To characterize the upper transition, the cell pressure is increased until the sample becomes cloudy, which is the transition point, then the pressure continues to increase, and the height of the two liquid phases is recorded by the cathetometer. After separation, volumetric data of the phases is taken up to 7 MPa above the transition point. Once the upper transition has been completed, the cell is slowly depressurized, as the large amount of $CO_2$ can cause the glass tube to rupture, up to 34.5 MPa, with no volumetric data taken at this stage. Afterwards, the cell continues to be depressurized, now recording volumetric data. At this stage, the lower liquid-liquid transition point, the density inversion and the lower liquid-liquid transition point will be found during pressure reduction; i) LL transition point, ii) the barotropic inversion region, and finally the liquid-liquid-vapor three-phase point.

Once all the transitions to the current $CO_2$ content have been determined, the pressure is raised to 27.6 MPa and a new injection of $CO_2$ is made to increase the existing quantity, resulting in a mixture with a higher $CO_2$ concentration. Then a new measurement process begins, using the same experimental procedure, as described. Each test provides the following results: sample transition pressure (bubble pressure or dew pressure); relative volume (ratio between the volume occupied by the fluid at any pressure and the volume occupied at any pressure and the volume occupied at saturation pressure); volume of the liquid and/or gaseous phases at the measured pressure and at saturation pressure; and the specific mass of the sample above when single-phase. In this paper, the transitions and the atypical behaviors are reported and discussed. Future publications will report density/volumetric data.

## Results and Discussion

With optimum pressure-temperature control of the equipment, it was possible to map out the miscibility window of the binary mixture of n-$C_{16}H_{34}$ and $CO_2$ at 298K, as shown in fig. (3).

The points shown in fig. (3) filled in solid black are not experimental data from this work. This data for both the upper and lower L-LL transition was taken from the literature [3, 4] in order to plot the miscibility window curve.

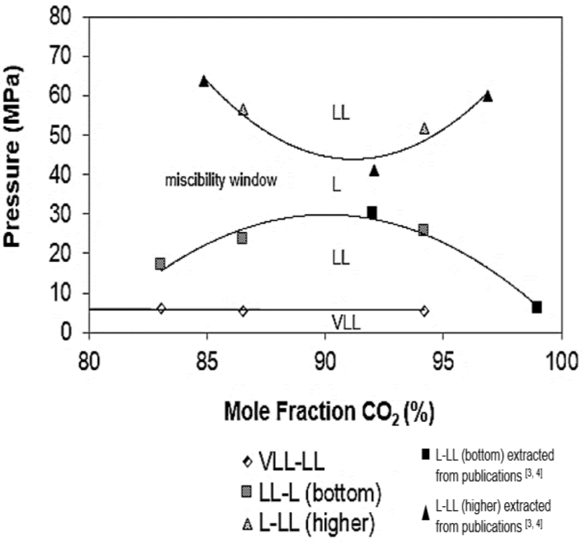

Figure 3. P-x diagram of $CO_2$ and n-$C_{16}H_{34}$ system at 298 K
Source: elaborated by the author (2024)

Figure 1 shows regions of two liquid phases at high pressures and high $CO_2$ contents, which is somewhat different from the usual liquid-liquid phase behavior. This special phase behavior can only be tracked by the apparatus in the vicinities of the temperature investigated in this paper. In this study, it was possible to observe this behavior at 86.53% and 94.18% molar of $CO_2$ in n-Hexadecane.

These LL regions of the graph are characterized by two dense phases and has been little investigated in the literature. The separation of the phases is usually slow in these regions due to the low interfacial tension between them and the small difference in specific mass.

However, in the vicinities around LL limits, there was no phase separation over a sufficiently long period of time at constant pressure. In practice, the phase transition was observed by the cloudiness of the sample contained in the cell and it remained cloudy even when the pressure was increased (in the case of the upper L to $L_1L_2$ transition) or reduced (in the case of the lower L to $L_1L_2$ transition) until the two liquid phases finally separated. The pressure range in which one phase dispersed into the other varied according to the content of $CO_2$ mixed with n-$C_{16}H_{34}$, as shown in Tables 1 and 2.

It is possible to infer how difficult the process of separating the incipient phase from the pre-existing phase is, both for the lower and upper liquid-to-liquid transfer. In comparison, the separation of the phases is more resistant to the pressure value inside the upper transition, due to the effect of the lower interfacial tension between the phases at higher pressure values. In the lower transition, the effect of the density of the phases is more representative, where the density of CO2 is close to that of C16, making it difficult to separate the CO2-rich phase from the C16-rich phase. The density of CO2 is more reflective of the variation in pressure to which it is subjected, while the density of C16 varies on a relatively smaller scale with pressure.

Table 1. Upper phase transition pressure data for the n-$C_{16}H_{34}$ system with high $CO_2$ content

| **$CO_2$ content (%)** | **Upper L-$L_1L_2$ Transition Pressure (MPa)** | **Upper L-$L_1L_2$ Pressure Range Without Phase Separation (MPa)** |
|---|---|---|
| 57.14 | - | |
| 83.06 | - | |
| 86.53 | 56.6 | 56.6 to 61.4 |
| 94.18 | 51.7 | 51.7 to 54.5 |

Source: elaborated by the author (2024)

Table 2. Lower phase transition pressure data for the n-$C_{16}H_{34}$ system with high $CO_2$ content

| **$CO_2$ content (%)** | **Lower L-$L_1L_2$ Transition Pressure (MPa)** | **Lower L-$L_1L_2$ Pressure Range Without Phase Separation (MPa)** |
|---|---|---|
| 57.14 | - | - |
| 83.06 | 16.9 | 16.9 to 7.1 |
| 86.53 | 23.5 | 23.484 to 22.9 |
| 94.18 | 25.5 | 25.517 to 24.3 |

Source: elaborated by the author (2024)

Tables 1 and 2 show the pressure values for transitions from a single-phase system (liquid) to a two-phase system (two liquids) above and below the miscibility window. The pressure range in which there is no phase separation is also shown. An important finding is that the lower the $CO_2$ content within the range in which there is a transition from L to $L_1L_2$, the more difficult it is to separate the phases. In other words. at 86.5% there was a greater pressure interval between the transition and the actual phase separation than when 94.18% $CO_2$ was added to the n-hexadecane. Fig. (4) illustrates the sample in the cell between 56.565 and 61.384 MPa where there is no phase separation even though the transition has already occurred. All the images from the range mentioned in Tables 1 and 2 are visually characterized by a high level of turbidity which was not seen when it was single-phase, and which becomes transparent again when it leaves the phase separation range.

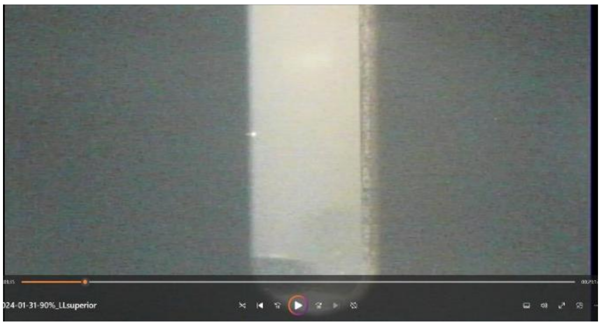

Figure 4. Image of the system with 86.53% $CO_2$ at a pressure between 56.565 and 61.384 MPa in which there was no phase separation in the upper liquid-liquid transition.

A relevant occurrence observed during the experiment was the position of the incipient phase in the cell after phase separation had taken place. In the P-x diagram, the experiments with the $CO_2$ content to the left of the critical point had a different distribution of phases from that to the right of the critical point, in this case 94.18% $CO_2$.

In the tests with content to the left of the critical point (83.06% and 86.53% $CO_2$), (LL “bubble point”) the incipient phase was at the bottom of the cell, where the phase with the lowest molar mass appears. In the test to the right of the critical point (94.18% $CO_2$) (LL “dew point”), the phase with the higher molar mass was in the upper part of the cell. In view of that, it can be concluded that for the latter content (94.18%), the incipient phase is less dense and rich in $C_{16}$. At lower $CO_2$ contents (86.53%), the incipient phase is denser (it is in the bottom) with a lower molar mass and it is richer in $CO_2$. Accordingly, the phase at the top is rich in $C_{16}$. Fig. (5) shows a schematic representation of this phase separation behavior. This characteristic, which is the opposite from what is normally expected, is due to the high density shown by $CO_2$ at high-pressures.

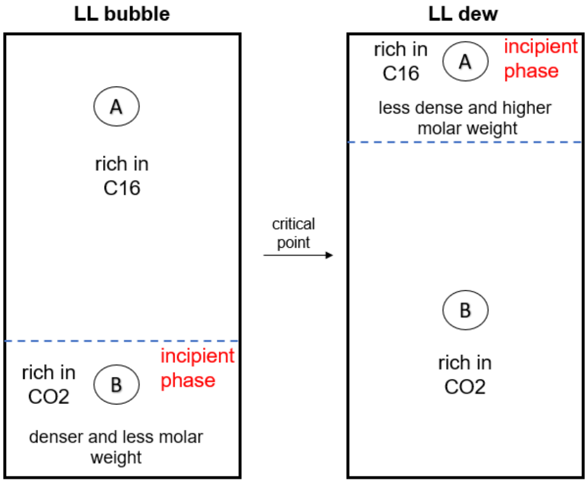

Figure 5. Diagram of the position of the incipient phase depending on the $CO_2$ content in the system. indicating the position in relation to the critical point on the P-x diagram.
Source: elaborated by the author (2024)

Another phenomenon observed during the experiment was the barotropic inversion. In the PVT test carried out, it is characterized as the pressure at which the density of the $CO_2$-rich phase became lower than that of the $C_{16}$-rich phase during depressurization, causing the reversal of the positioning of the phases shown in fig. (5). This is due to the fact that the density of $CO_2$ varies greatly according to the pressure at which it is confined. Therefore, this happens when the density values of the two components of the mixture are very close, what is shown in fig. (6). The phases are in continuous movement towards each other at constant pressure, until a small reduction in pressure causes the positions to reverse. At pressures below the point of barotropic inversion, the $CO_2$-rich phase is above the $C_{16}$-rich phase. In all the tests, regardless of the $CO_2$ content, the barotropic inversion occurred at around 8.96 MPa.

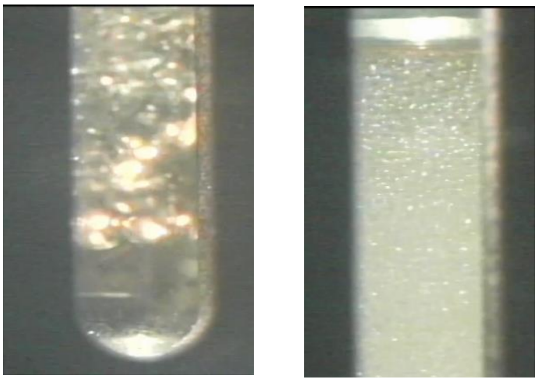

Figure 6. Barotropic inversion occurred in the tests with 86.53% and 94.18% $CO_2$ to the left and right, respectively.

## Conclusions

The main conclusions of the work are depicted bellow:

- In these experiments, the lower the $CO_2$ content in the interval in which the transition from L to

$L_1L_2$ took place, the more difficult the phase separation was. In other words, at 86.5% of $CO_2$ composition, there was a greater pressure interval between the transition and the actual phase separation than 94.18% $CO_2$ system;

- A region close to the system's critical point was identified, where the $CO_2$ mole fraction was around 94%. The pressures of the LL critical points were around 25.5 and 51.7 MPa for the lower and upper transition, respectively. Determining the exact critical point experimentally is impossible, requiring extrapolation or modeling, which suggests areas for future research;
- In the tests where the $CO_2$ content was to the left of the critical point (83.06% and 86.53% $CO_2$), the incipient phase was in the lower portion of the cell (phase with a lower molar mass but denser). In the test to the right of the critical point (94.18% $CO_2$), the phase with the highest molar mass appeared in the upper portion of the cell;
- Barotropy was identified in the experiment. Regardless of $CO_2$ content, barotropic inversion occurred at around 8.96 MPa, above the LLV transition.

## Responsibility Notice

The authors are the only responsible for the paper content.

## References

[1] Green, D. W.; Willhite, G. P. *Enhanced Oil Recovery*. 2. ed., Richardson (TX, USA), SPE Textbook Series, 2018. 895 p.

[2] Stalkup JR, F. I. Miscible Displacement. New York (NY, USA): SPE of AIME, 204 p. 1983.

[3] Simoncelli. A. P.. Goméz. W.. Charin. R. M.. Fleming. F. P. Ndiaye. P. M.. & Tavares. F. W. Phase behavior of systems with high $CO_2$ content: Experiments and thermodynamic modeling. *Fluid Phase Equilibria*. 2020. *515*. 112574.

[4] Schneider. G. et al. Hasengleichgewichte und kritische Erscheinungen in binären Mischsystemen bis 1500 bar. $CO_2$ mit n-Octan. n-Undecan. n-Tridecan und n-Hexadecan. *Chemie Ingenieur Technik*. 1967. *39* (11). 649-656.

[5] Stalkup, Fred I. Status of Miscible Displacement. *J Pet Technol* 35 (1983): 815–826.